Heliyon 10 (2024) e33131

Contents lists available at ScienceDirect

Heliyon

journal homepage: www.cell.com/heliyon

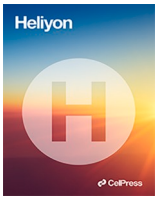

Research article

Early fetal sex determination using a fluorescent DNA nanosensing platform capable of simultaneous detection of *SRY* and *DYS14* sequences in cell-free fetal DNA

Saeed Mohebbi [a], Sheida Zoughi [b], Farnoush Faridbod [b], Sharif Moradi [a,c,*]

[a] *Department of Stem Cells and Developmental Biology, Cell Science Research Center, Royan Institute for Stem Cell Biology and Technology, ACECR, Tehran, Iran*
[b] *Center of Excellence in Electrochemistry, School of Chemistry, College of Science, University of Tehran, Tehran, Iran*
[c] *miRas Biotech, Tehran, Iran*

ARTICLE INFO

Keywords:
Carbon nanoparticle
Circulatory DNA
Nanobiosensor
Biomarker
Blood-borne marker

ABSTRACT

Early fetal sex determination is of crucial importance in the management of prenatal diagnosis of X-linked genetic abnormalities and congenital adrenal hyperplasia. The development of an efficient and simple method for high-sensitivity, affordable, and rapid screening of cell-free fetal DNA (cffDNA) is crucial for fetal sex determination in early pregnancy. In this study, single- and dual-fluorophore DNA biosensors based on multi-walled carbon nanotubes (MWCNT) were fabricated for the individual and simultaneous detection of the *SRY* gene and *DYS14* marker in cffDNA obtained from maternal plasma samples. This nanosensing platform is based on the immobilization of single-stranded DNA (ssDNA) probes, labeled with ROX or FAM fluorophores, on MWCNT, resulting in the quenching of fluorescence emission in the absence of the targets. Upon the addition of the complementary target DNA (ctDNA) to the hybridization reaction, the fluorescence emission of fluorophore-labeled probes was significantly recovered to 79.5 % for ROX-labeled probes (i.e. *SRY*-specific probes), 81.5 % for FAM-labeled probes (i.e. *DYS14*-specific probes), and 65.9 % for dual-fluorophore biosensor compared to the quenching mode. The limit of detection (LOD) for ROX, and FAM was determined to be 4.5 nM, and 7.6 nM, respectively. For dual-color probes, LOD was found to be 5.4 (ROX) and 9.2 nM (FAM). Finally, the clinical applicability of the proposed method was confirmed through the detection of both biomarkers in maternal plasma samples, suggesting that the proposed nanosensing platform may be useful for the early detection of fetal sex using cffDNA.

1. Introduction

Early fetal sex determination offers several advantages for parents such as peace of mind and allowing them to prepare for the arrival of their newborn. Moreover, it enables to check the health status of the fetus in prenatal diagnosis of X-linked genetic diseases such as hemophilia A and Duchene muscular dystrophy, as well as to monitor women at risk of having an infant with congenital adrenal hyperplasia [1,2]. Traditionally, fetal sex determination has been carried out either using invasive techniques such as

* Corresponding author. Royan Institute, Banihashem Sq., Banihashem St., Soleimani Highway, Tehran. Postal Code: 1665659911, P.O. Box: 16635-148, Iran.
E-mail addresses: sh.moradi@royan-rc.ac.ir, sharif.moradi@gmail.com (S. Moradi).

https://doi.org/10.1016/j.heliyon.2024.e33131
Received 24 January 2024; Received in revised form 28 May 2024; Accepted 14 June 2024
Available online 15 June 2024

amniocentesis or chorionic villus sampling (CVS), which carry a significant risk of miscarriage and intrauterine infection, and cannot be performed at early gestational ages, or non-invasively by ultrasonography [3,4]. However, the latter cannot be carried out reliably until the 11th week of pregnancy, because the external genitalia is not completely developed until this stage [4,5]. Therefore, there is a high demand for the development of an early procedure for sex determination in a highly sensitive, specific, and safe manner.

The initial discovery of circulating cell-free fetal DNA (cffDNA) fragments in the maternal plasma during pregnancy in 1997 has enabled to carry out non-invasive prenatal testing (NIPT) [6]. Fragments of cffDNA originate from apoptotic trophoblasts of the placenta in the maternal bloodstream and can be detectable from around 5 weeks in gestation [7], however, it can be reliably detected from 7 weeks of gestation [3]. The size of fetal DNA molecules is reported to be generally between 193 and 313 bp (typically shorter than 200 bp) [8,9], which comprise approximately 10% of total DNA present in maternal plasma [10,11]. Currently, the cffDNA-based methods for sex determination include quantitative real-time polymerase chain reaction (qPCR) [10], Digital PCR, and massively parallel sequencing [12], which detect the presence or absence of Y-chromosome-specific sequences, such as the single-copy *SRY* gene sequence, multi-copy *DYS14* marker sequence of the *TSPY* gene, and unique multi-copy regions of the Y chromosome, such as the DAZ family in the maternal plasma [13]. It would be of crucial importance to simultaneously detect both DNA markers, which has not previously been studied, to enhance the sensitivity and specificity of sex determination. The results of the various widely used detection methods have been encouraging, with their specificity and sensitivity ranging from 31% to 100% [14] depending on the strategy and method used. Despite their advantages, these methods still suffer from being time-consuming or requiring expensive instruments and reagents as well as expert operators. Therefore, developing a rapid, simple, and inexpensive sex-determination method is crucially important and highly favorable.

Recently, several attractive sensing strategies have been used for the detection of cell-free DNA (cfDNA) based on fluorescent, electrochemical, and colorimetric platforms [15–17]. Among them, fluorescence-based biosensors that utilize fluorescent DNA probes have attracted great attention due to their high sensitivity and selectivity, simplicity, rapidness, and cost-effectiveness [18,19]. The simplest fluorescence DNA sensing methods typically utilize a fluorophore and a quencher attached to the opposite ends of a DNA probe and work based on fluorescence resonance energy transfer (FRET) between fluorophore and quencher (a quenching mechanism). The binding of target DNA induces the dissociation of quencher and fluorophore, allowing fluorescence recovery [20,21].

Despite the widespread use of fluorescent biosensors for the detection of nucleic acids, they still suffer from the need for careful selection of fluorophore and quencher pairs in order to achieve optimum efficiency. Recently, nanomaterials have been used as quenchers to address this challenge since they can quench a variety of fluorophores with varying emission wavelengths while improving signal-to-noise ratio [22–24]. Among these nanomaterials, graphene oxide [25], carbon quantum dots [20], gold nanoparticles [26,27], metal−organic frameworks [28], and carbon nanotubes [21,29] have been adopted as efficient nano-quenchers to develop fluorescent biosensors for detection of various biomarkers such as nucleic acids and proteins.

Carbon nanotubes, including single-walled carbon nanotubes (SWCNTs) and multi-walled carbon nanotubes (MWCNTs), have played major roles in biosensor development due to their unique structural, optical, and electrical characteristics. They have various unique features such as large surface area, high stability, easy functionalization and preparation, biocompatibility, low cytotoxicity, and strong fluorescence quenching of dye molecules through FRET mechanism [30,31].

These studies focus on the effective utilization of MWCNTs, particularly when attached through covalent or noncovalent bonds with nucleic acids. Notably, the noncovalent interaction of single-stranded DNA (ssDNA) with MWCNTs has been a subject of recent interest. The stable complexes formed by ssDNA and MWCNTs involve intricate π-stacking interactions between nucleotide bases and the sidewalls of MWCNTs [21]. Initially, ssDNA molecules encircle individual MWCNTs through π-stacking interactions occurring between the nucleotide bases and the sidewalls of the MWCNTs. Following this interaction, owing to the dual role of MWCNTs as a "nanoscaffold" for ssDNA and a "nanoquencher" of the fluorophore, only one end of the ssDNA needs to be tagged with a fluorophore. In this scenario, the ssDNA molecules organize themselves on the carbon nanotube surface, leading to complete quenching of the

Table 1
The DNA sequences used in this study.

Oligo Name	Oligo Sequence (5'→3')	Oligo Type
SRY sequences		
SRY-Lprobe	5'-ROX-GGACTCTGAGTTTCGCATTCTCAGAG-3'	Probe
cDNA	5'-AGAATGCGAAACTCAGAG-3'	Target DNA
mDNA (1 nt)	5'- AGAATGCGACACTCAGAG-3'	Mismatch target DNA
mDNA (3 nt)	5'- AGACTGAGACACTCAGAG-3'	Mismatch target DNA
mDNA (5 nt)	5'- AGAGTGAGACACTCCGCG-3'	Mismatch target DNA
ncDNA	5'-AGCTGGGATACCAGTGGA-3'	Non-complementary DNA
SRY-F	5'-AAAGGCAACGTCCAGGATAGAG-3'	Forward primer
SRY-R	5'-TGAGTTTCGCATTCTGGGATT-3'	Reverse primer
DYS14 sequences		
DYS14-Lprobe	5'-FAM-TCTAGTGGAGAGGTGCTC-3'	Probe
cDNA	5'-GAGCACCTCTCCACTAGA-3'	Target DNA
mDNA (1 nt)	5'-GAGCAACTCTCCACTAGA-3'	Mismatch target DNA
mDNA (3 nt)	5'-GAGCACCTTTCAACTAAA-3'	Mismatch target DNA
mDNA (5 nt)	5'-AAGCGCCTTTCAACTAAA-3'	Mismatch target DNA
ncDNA	5'-GATTCCACGGCTGTCAAC-3'	Non-complementary DNA
DYS14-F	5'-GGGCCAATGTTGTATCCTTCTC-3'	Forward primer
DYS14-R	5'-AAGAGTCACATCGACGCCGAG-3'	Reverse primer

fluorophore. Subsequently, when a target is present, competitive binding between the target and the carbon nanotubes with the ssDNA disrupts the fluorescence quenching, thereby enabling enhancement of the fluorescence signal [21,32].

In this study, we develop stem-loop-probe and linear-probe fluorescent DNA sensors based on MWCNTs for individual as well as simultaneous detection of the DNA markers *SRY* and *DYS14* for fetal sex determination using cffDNA. We show that this platform enables the accurate determination of fetal sex based on 14 clinical samples from pregnant women at an early gestational age, i.e. 8−37 weeks. We further demonstrate that our biosensor accurately detects male cffDNA in the plasma of pregnant women. Overall, our nanobiosensing platform provides a highly selective, sensitive, specific, and cost-effective tool for fetal sex determination.

2. Experimental section

2.1. Materials and apparatus

All reagents, including Tris hydrochloride (Tris-HCl, >99%), sodium chloride (NaCl, >99%), potassium chloride (KCl, >99%), and magnesium chloride ($MgCl_2$, ≥97.0%) solutions were purchased from Sigma-Aldrich (Singapore), unless otherwise stated. The Tris-HCl buffer solution (20 mM) was used in the presence of 100 mM NaCl, 5 mM KCl, and 5 mM $MgCl_2$. pH 7.4. Stock solutions were prepared using sterilized double-distilled water (SDDW). The designed DNA oligonucleotides used in this study (Table 1) were synthesized and purified by miRas Biotech (Tehran, Iran). BLAST searches were performed to ensure that the stem-loop- and linear-probe-based fluorescent DNA sensors only recognized sequences in the *SRY* gene and *DYS14* marker and that they do not detect any other homologous sequences in human genomic DNA. All oligonucleotides were dissolved in TE buffer (10 mM Tris, 1 mM EDTA, pH 7.2), and the resulting solutions were kept frozen at −20 °C. The circulating plasma DNA was isolated from maternal blood samples using the NucleoSpin cfDNA XS kit (Düren, Germany). A FavorPrepTM Blood Genomic DNA Extraction Mini Kit from Favorgen (Ping-Tung, Taiwan) was used to extract DNA from male blood samples in order to serve as positive controls. MWCNTs were obtained from US Research Nanomaterials, Inc. The size and morphology of the MWCNTs were examined by field emission scanning electron microscopy (FESEM, HITACHI S4160 microscope), Energy-dispersive spectroscopy (EDX, HITACHI S4160 microscope), and Fourier transform infrared spectroscopy (FT-IR, Bruker, USA - Tensor 27) analyses. A fluorescence spectrophotometer (Varian Cary Eclipse) was used for fluorescence measurements of ROX-labeled probes (ROX-Lprobe; excitation at 578 nm and emission scanning at 605 nm) and FAM-labeled probes (FAM-Lprobe; excitation at 495 nm and emission scanning at 520 nm) at room temperature.

2.2. Obtaining cffDNA samples from maternal plasma

Whole blood samples in EDTA vacutainer tubes were collected from 14 pregnant women volunteers between 8 and 37 weeks of gestation, with 11 male-bearing pregnancies provided by Shohada-Miandoab Clinic (Iran). To obtain plasma from the blood samples, 5 mL of fresh peripheral blood from each individual was centrifuged at 604×*g* (4 °C, 10 min), followed by the centrifugation of the supernatant at 6764×*g* (4 °C, 3 min). cffDNA was isolated from plasma samples using the NucleoSpin® plasma XS Kit (Düren, Germany) according to the manufacturer's instructions, followed by DMSO treatment to denature the double-stranded DNA.

The isolated DNA was stored at −80 °C until further study. Two μL of the extracted cfDNA was analyzed by traditional PCR assays specific for the *SRY* gene (Forward: 5′-AAAGGCAACGTCCAGGATAGAG-3′; Reverse: 5′-TGAGTTTCGCATTCTGGGATT-3′) and *DYS14* marker (Forward: 5′-GGGCCAATGTTGTATCCTTCTC-3′; Reverse: 5′-AAGAGTCACATCGACGCCGAG-3′) to pre-amplify and quantify the cffDNA, in case of a male fetus. To detect the specific sequences of *SRY* and *DYS14* markers in the cffDNA samples extracted from the maternal plasma, 50 μL cffDNA was added to the fabricated biosensor (MWCNTs-ssDNA conjugate under optimized condition), and after 28 min of incubation, the detection procedure was carried out to determine the recovery rate of fluorescence emission. Each reaction had a final volume of 25 μL and was done in duplicates. Standard male genomic DNAs were obtained from seven male individuals to serve as positive controls. No-template controls were also included in the study. The reactions were carried out on a DNA amplifier (Eppendorf Master-cycler Gradient Thermal Cycler) according to the following amplification program: 2 min at 50 °C, 10 min at 95 °C, 50 amplification cycles comprising a denaturation step at 95 °C for 30 s, an annealing-elongation step at 58 °C for 1 min, and extension step at 72 °C for 1 min. The study was approved by the Ethics Committee of the Royan Institute, Tehran, Iran. All pregnant women involved in the study signed an informed consent form and were completely aware that the study is a research project for determining fetal sex.

2.3. Fabrication and characterization of DNA Probe-MWCNT conjugates

To fabricate the MWCNT-based biosensing platform, we first prepared MWCNT-DNA conjugates, in which the MWCNT nanoparticles quench the fluorescence emission of fluorophore-labeled single-stranded DNA (ssDNA) oligonucleotides (ROX/FAM-Lprobe). For the preparation of MWCNT-ssDNA conjugates, 10 μL (10 μmol/L) of the ssDNA probe was added to 10 μL (1 mg/mL) of MWCNT. Next, the resulting solution was adjusted to 500 μL with Tris-HCl buffer (pH 7.4) while vortexing. Then, to completely cover the MWCNT surface with ssDNA probes, the conjugate solution was incubated at different times for up to 30 min at room temperature. The Varian Cary Eclipse Fluorescence Spectrophotometer was used to record fluorescence intensity changes. The measurement was performed using a quartz fluorescence cell with an optical path length of 1.0 cm. The emission spectra for ROX-Lprobe were recorded from 580 to 700 nm with excitation at 575 nm, and for FAM-Lprobe from 500 to 650 nm with excitation at 494 nm. In both cases, the slit widths of the excitation and emission were set to 5 and 10 nm, respectively. The quantitative assays of the fluorescence intensity for ROX- and FAM-L probes were carried out at 605 and 520 nm, respectively. To confirm the properties of MWCNT-ssDNA conjugates,

characterizations were performed with FESEM (HITACHI S4160 microscope), EDX (HITACHI S4160 microscope), and FT-IR (Bruker, USA - Tensor 27) analyses.

2.4. Investigation of the quenching efficiency

To determine the optimum concentration of MWCNT for efficient quenching of the fluorophore-labeled ssDNA probes (ROX- and FAM-Lprobe), different concentrations of MWCNT (5–80 μg) were added to solutions containing 10 μL of 10 μM ROX- or FAM-Lprobe. In all cases, the total volume of the reaction solution was 500 μL in 20 mM Tris-HCl buffer solution, pH 7.4. After incubation at optimum absorption time, the fluorescence was measured by Varian Cary Eclipse Fluorescence Spectrophotometer. At the optimal MWCNT concentration, the fluorophore-labeled DNA typically remains less free in solution and therefore the fluorescence emission is further reduced.

2.5. Optimization of the DNA detection conditions

After the preparation of optimized MWCNT-ssDNA conjugates, hybridization experiments were performed in a 20 mM Tris-HCl buffer solution, pH 7.4, with a series of complementary target DNA (ctDNA) molecules with different concentrations. First, 50 μL of the MWCNT-ssDNA conjugate solution was mixed with 10 μL of ctDNA (10 μmol/L), the resulting mixture was transferred to a cuvette, and the fluorescence intensity emission was measured at different incubation times (1–30 min) at room temperature. Next, the mixture was allowed to hybridize to ctDNA for ~30 min at room temperature. A series of hybridization solutions with various amounts of ctDNA (0.4, 2, 4, 20, 40, 100, 200, 300, 400, 500, 600, 700, 800, 900, and 1000 nM) was used to determine the optimal hybridization time and the biosensor sensitivity. To analyze the specificity of the biosensor, we evaluated the fluorescence response induced by ctDNA, a non-complementary DNA (ncDNA) target, and DNA targets containing single or three mismatches. The limit of detection (LOD) for the sensitivity of the biosensor was defined as the minimum concentration of ctDNA that significantly shows detectable fluorescence emission compared to the quench mode.

2.6. Multiplex simultaneous detection of DNA with multicolor fluorescent biosensor

The hybridization experiments for the multiplexed detection of DNA were carried out by mixing 15 μL of 10 μM ROX-Lprobe or FAM-Lprobe with 20 μL of MWCNT in a Tris-HCl buffer solution, such that the final volume of the hybridization reaction solution was kept constant at 500 μL. Next, the ssDNA probe-MWCNT conjugates were incubated at different times (0–28 min) to assay the adequate absorption of the probe on the surface of the MWCNTs, and fluorescence intensity changes were measured by synchronous scanning fluorescence spectrophotometer. The intervals between the maximum excitation and emission wavelengths of ROX and FAM are known to be 24 nm and 26 nm, respectively.

In order to achieve the simultaneous quenching of the two fluorophores, the fixed wavelength difference (Dλ) of synchronous scanning spectrofluorometric is set at 25 nm. To optimize the concentration of MWCNTs for complete quenching of the ROX-Lprobe and FAM-Lprobe, different concentrations of MWCNTs were mixed with 20 μL from ROX/FAM-Lprobe and then the fluorescence intensity quenching was measured by spectrofluorometry at the optimum absorption time.

After the fabrication of MWCNT-based dual-color fluorescent biosensor, a hybridization reaction was conducted with different amounts of ctDNA. First, 20 μL of each ctDNA (10 μmol/L) was mixed with optimized MWCNT-ssDNA conjugate solution, and fluorescence emission was then investigated at different incubation times (1–38 min) at room temperature. After the determination of the optimized hybridization time, the optimization of the amount of ctDNA was carried out with various amounts of target sequence, with final concentration ranging from 10 nM to 2 μM.

2.7. Statistical analysis

All fluorescence emission measurement experiments were carried out in triplicates. The results are expressed as mean ± SD. Statistical analysis was done with GraphPad Prism software version 9.0 and the significance level was considered at $p < 0.05$.

3. Results and discussion

3.1. Immobilization of single-stranded fluorophore-labeled DNA probes on MWCNTs

First, we tried to non-covalently immobilize fluorophore-labeled ssDNA probes on MWCNT. Since ssDNA is a polyanion, interactions between DNA and MWCNT appear to be through strong intermolecular hydrophobic π-π* interaction, electrostatic repulsion, and hydrogen bonding. In the absence of MWCNT, we observed a strong fluorescence emission related to ROX and FAM fluorophores attached to ssDNA probes at 605 and 520 nm, respectively. However, adding MWCNT led to a gradual decrease and quenching of the fluorescence emission at room temperature (Fig. S1 in the Supporting Information), suggesting strong interaction between MWCNT and ROX- and FAM-labeled ssDNA probes as well as the high fluorescence quenching ability of MWCNT. This is because when the fluorophores are placed in the proximity of MWCNT upon conjugation and ROX and FAM fluorophores are excited at 495 and 576 nm, respectively, they transfer the energy to the MWCNT through FRET [21], which results in the quenching of the fluorescence signal of the fluorophores. We investigated the kinetics of fluorescence quenching of ROX- and FAM-Lprobe by MWCNT

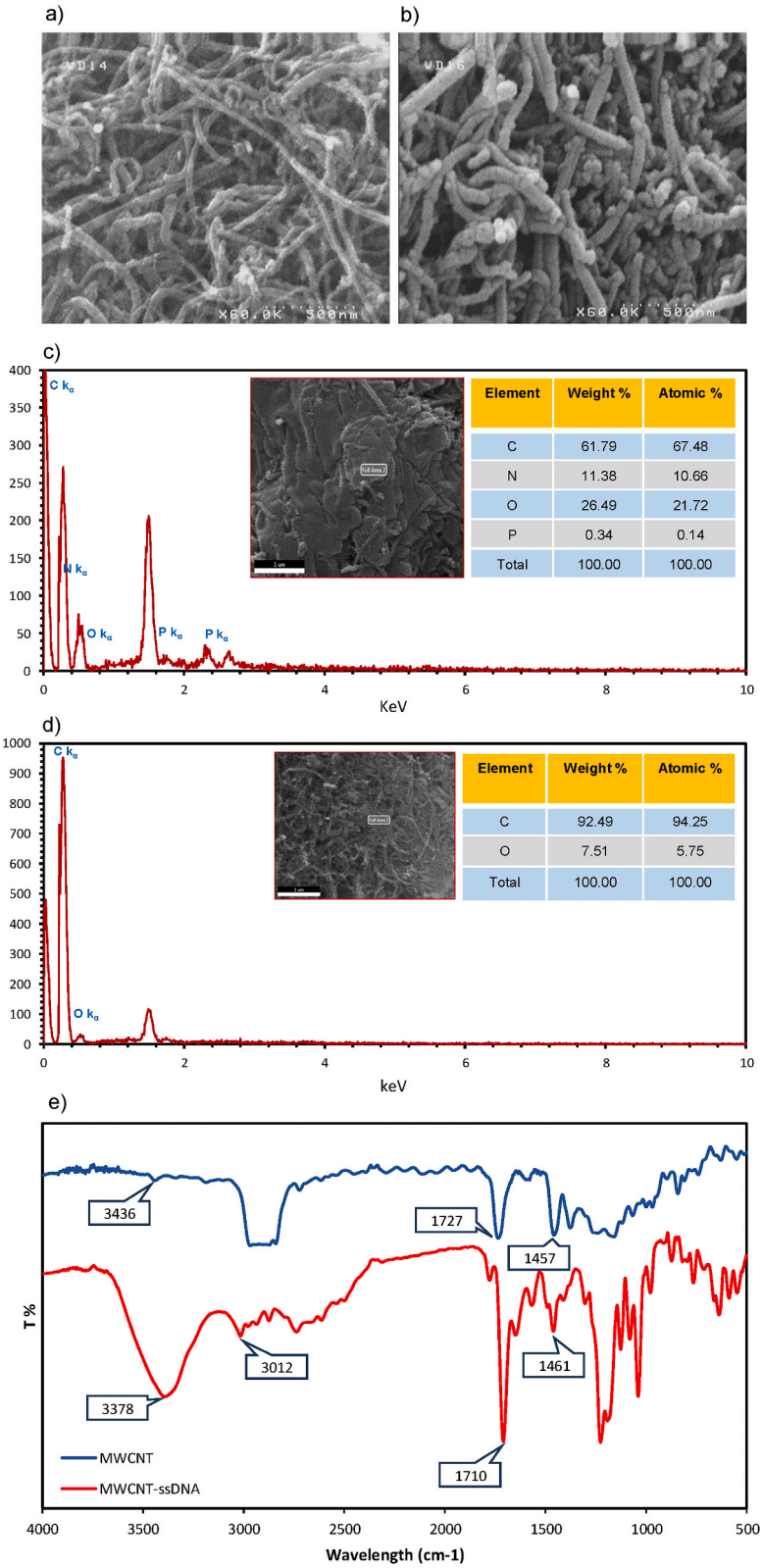

Fig. 1. Characterization of the MWCNT-ssDNA Conjugates. FESEM images of MWCNTs (a) and MWCNT-ssDNA Conjugates (b). (c) EDX spectrum of MWCNTs. (d) EDX spectrum of fluorophore-labeled ssDNA-MWCNT conjugates. (e) FT-IR spectra of MWCNT and ssDNA-MWCNT conjugates.

by measuring fluorescence intensity at different incubation times. As shown in Fig. S2, upon addition of MWCNT to the solution of ROX- or FAM-labeled ssDNA, the fluorescence emission intensity greatly decreased within the first 2 min. Then, the fluorescence intensity was further decreased for both ROX- and FAM-labeled ssDNA probes with an increase in quenching time. Finally, the fluorescence intensity reached a steady value after 10 min (ROX-Lprobe) or (FAM-Lprobe) (Figs. S2a–d). Therefore, after 10 min, most of the sites at the MWCNT surface are covered by ROX-Lprobe and FAM-Lprobe, respectively, indicative of the rapid quenching kinetics of MWCNT. These times were estimated as functional quenching times for the fluorophore-labeled probes.

Next, we investigated the kinetics of simultaneous quenching of the two fluorophores' fluorescence by MWCNTs through

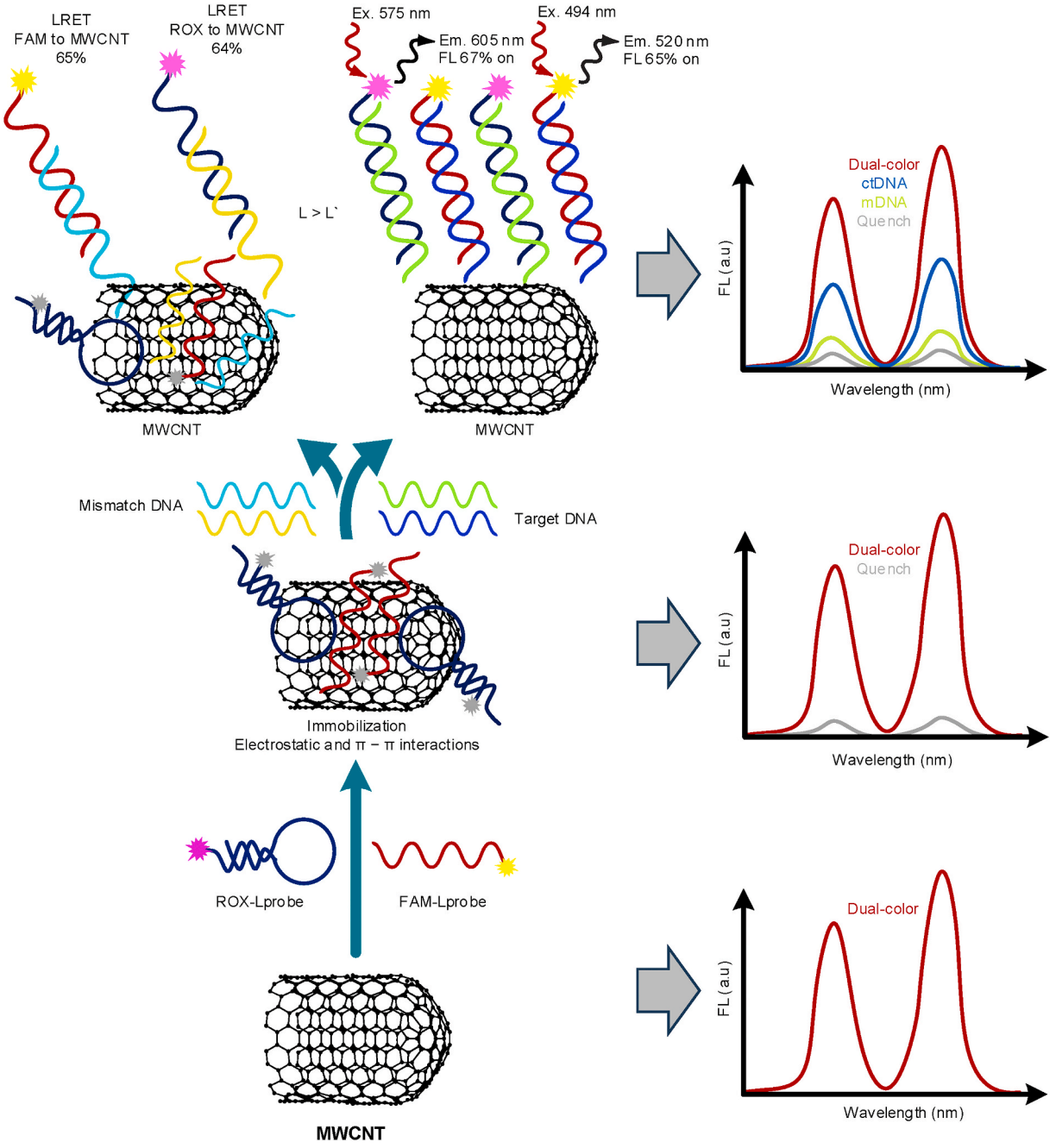

Fig. 2. Schematic Illustration of MWCNT-Based Fluorescent Detection of DNA. This platform is based on the adsorption of fluorophore-labeled ssDNA probes, i.e. ROX/FAM-Lprobes, onto the MWCNT, leading to fluorescence quenching. In contrast, when ROX- or FAM-Lprobe hybridizes to corresponding ctDNA to form a duplex DNA structure (i.e. dsDNA), the interactions between dsDNA and MWCNT becomes weakened such that the dsDNA is desorbed from the MWCNT surface, leading to the restoration of the fluorescence of ROX- and FAM-Lprobes.

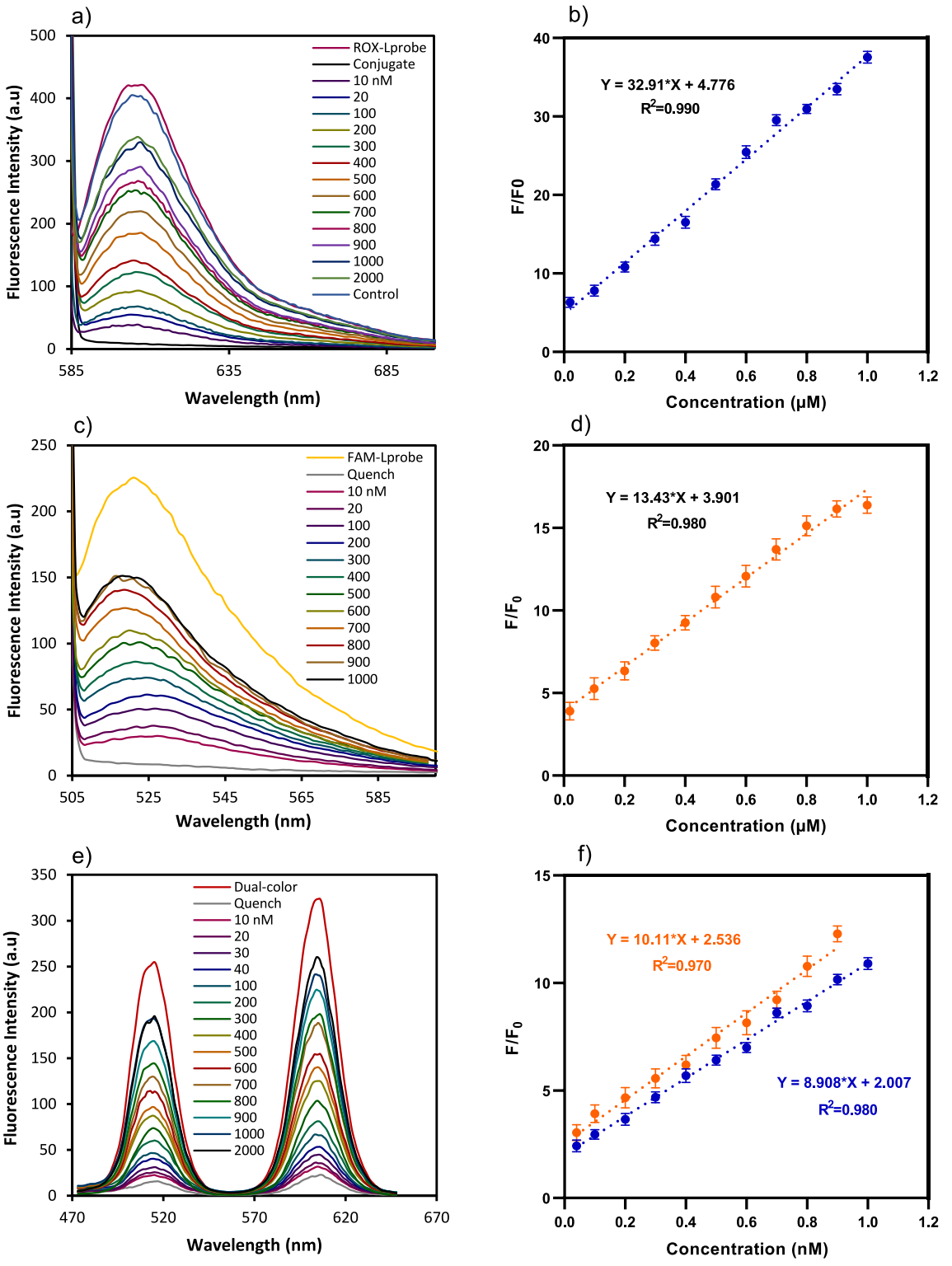

(caption on next page)

Fig. 3. Corresponding Fluorescence Emission Spectra in the Presence of Different Concentrations of ctDNA and Calculation of the Calibration Curve. Fluorescence emission spectra restoration of ROX-Lprobe (a), FAM-Lprobe (c), and dual-color (e) upon ctDNA hybridization in the presence of different concentrations of ctDNA (0.4, 2, 20, 40, 200, and 400 nM). Calibration curves for the detection of DNA hybridization based on MWCNT for ROX-Lprobe (b), FAM-Lprobe (d), and dual-color biosensor (f). F0 and F indicate the fluorescence intensity of the biosensor in the absence and presence of ctDNA, respectively. The data were recorded with excitation and emission wavelengths of 495 and 520 nm (FAM-Lprobe) and 578 and 605 nm (ROX-Lprobe), respectively. (For interpretation of the references to color in this figure legend, the reader is referred to the Web version of this article.)

measuring fluorescence intensity at different incubation times. As shown in Fig. S2e, both ROX- and FAM-Lprobe were simultaneously immobilized on the MWCNTs 16 min post-incubation. In another experiment, different amounts of MWCNTs were evaluated at the optimal quenching time to find an MWCNT concentration at which the complete quenching of fluorescence emission of both fluorophores occurs. We found that with increasing concentrations of MWCNTs, a decrease in the fluorescence intensity is observed (see Fig. S1). At a concentration of 50 μg/mL, more than 97% of the ROX fluorescence, at a concentration of 60 μg/mL, more than 95% of the FAM fluorescence, and at a concentration of 80 μg/mL, more than 90% of the dual ROX/FAM-Lprobe fluorescence was quenched. The quenching efficiency of the ROX and FAM fluorescence reached 97.9 ± 0.6% and 95.8 ± 0.8%, respectively.

3.2. Characterization of the ssDNA-MWCNT conjugates

Preparation of *SRY*- and *DYS14*-specific ssDNA biosensors was carried out by immobilization of ssDNA probes on MWCNTs. To confirm the proper preparation of MWCNT-ssDNA conjugates, FT-IR, FESEM, and EDX analyses were carried out. FESEM analysis confirmed the expected morphological properties of MWCNTs and ssDNA-MWCNT conjugates (Fig. 1a and b). The morphological analysis of MWCNT by FESEM revealed turf and mat structures characteristic of these nanomaterials (Fig. 1a). FESEM analysis of ssDNA-MWCNT conjugates showed changes in the morphology and diameter of MWCNTs which confirms immobilization of ssDNA probes on MWCNTs (Fig. 1b). In addition, EDX confirmed the presence of ssDNA molecules immobilized on MWCNTs (Fig. 1c and d). In EDX analysis of ssDNA-MWCNT conjugates, the automatic assignments of C, O, N, and P elements suggested that ssDNA probes were successfully anchored to MWCNT, as P and N element signals, related to fluorophore-labeled ssDNA probes, were observed at around 2 and 0.5 KeV, respectively (Fig. 1d). From the FTIR spectra of MWCNT in Fig. 1e, the following bands were observed: stretching vibration of O–H groups as a peak at 3436 cm^{-1}, C═O vibrations at 1727 cm^{-1}, C═C stretching at 1457 cm^{-1}, and C–O vibrations at 1160 cm^{-1}. From the FTIR spectra of MWCNT-ssDNA, we observed a broad peak at 3378 cm^{-1} for O–H stretching modes of the –COOH groups and 3012 cm^{-1} for N–H of amide moieties (Fig. 1e). Other peaks appeared at 1710 cm^{-1} corresponding to stretching vibrations of C═O groups of unreacted carboxylic acids. Finally, a peak at 1710 cm^{-1}, which appeared as a shoulder on C═C vibrations at 1461 cm^{-1}, was also observed and attributed to the C═O vibration of amide moieties [20,33]. These data indicate that characteristic ssDNA probe-MWCNT conjugates were formed successfully and properly.

3.3. The fluorescent DNA biosensor efficiently detects ctDNA in ctDNA/mtDNA mixtures

To achieve the best sensing performance in the hybridization reaction, we optimized the two parameters of hybridization incubation time and different amounts of ctDNA in a Tris-HCl buffer solution. An illustration of multiplexed detection of DNA by a dual-color fluorescent biosensor based on MWCNTs is depicted in Fig. 2.

In the hybridization experiment, the kinetics of fluorescence recovery was investigated by measuring fluorescence emission intensity at different hybridization incubation times. As illustrated in Fig. S3, it was found that in the presence of 10 μL ctDNA (10 μM), the fluorescence intensity was rapidly enhanced during the first 5 min (resulting from rapid dsDNA formation following ssDNA desorption from MWCNT surface), and then with increasing incubation time, fluorescence intensity was further increased albeit less quickly (resulting from formation of more dsDNA) until it reached its maximum value without further change (resulting from saturation of the biosensor) after ~15 min. Therefore, the hybridization time of 13 min (ROX-Lprobe), 12 min (FAM-Lprobe), and 16 min (dual-color simultaneous) was considered as the optimal hybridization time.

Furthermore, a calibration experiment with different amounts of ctDNA was performed to investigate the range of detection for MWCNTs. As plotted in Fig. 3, with increasing concentration of ctDNA, enhancement in fluorescence emission intensity is observed. This can be explained by the fact that as the concentration of ctDNA increases, a higher degree of DNA hybridization occurs and more dsDNA is formed, so that less adsorption occurs on the MWCNT surface, resulting in lesser quenching and leading to high restoration of fluorescence emission of ROX- and FAM-Lprobe. Furthermore, different concentrations of ctDNA resulted in different intensities of ROX- and FAM-Lprobe emission fluorescence, thus quantitative determination of ctDNA could be achieved according to the ROX- and FAM-Lprobe fluorescence emission intensity. Based on this phenomenon, we have used the equation below to calculate the percentage restoration. % fluorescent restoration = (Ft-Fb)/(Fc-Fb) × 100; where Fb is the fluorescence signal of the buffer, Fc is the fluorescence signal of the ROX- or FAM-Lprobe containing buffer medium, and Ft is the fluorescence signal observed in the presence of a given concentration of ctDNA.

The dynamic range of detection was determined to be 0.01−1 μM for ROX-Lprobe and 0.02–1 μM for FAM-Lprobe. Experimental results revealed that a concentration of 1 μM of ctDNA could provide a maximum signal-to-background ratio (SBR) for the DNA sensing platform (Fig. 3a–d), and this value was chosen as the optimized conditions for further investigation. Of note, we also used mismatch DNA oligonucleotides as negative controls to evaluate the selectivity and specificity of the biosensor for *SRY* and *DYS14* markers. Furthermore, the sensitivity of the biosensor was evaluated with different amounts of ctDNA and LOD was calculated to be 4.5 nM (S/

Table 2
Optimization of the nanobiosensor.

Analyte	Bimolecular probe	Donor, Ex/Em [nm]	Quench time	MWCNT concentration	MQE[a]	Quenching mechanism	Assay Time (HCR)	cDNA concentration	LOD
SRY gene	Stem-loop-probe	ROX, 587/609	10 min	50 μg	~98%	Electrostatic and π–π interactions	13 min	1 μM	~4.5 nM
DYS14 marker	DNA probe	FAM, 494/521	10 min	60 μg	~96%	Electrostatic and π–π interactions	12 min	0.9 μM	~7.6 nM

[a] MQE: maximum quenching efficiency.

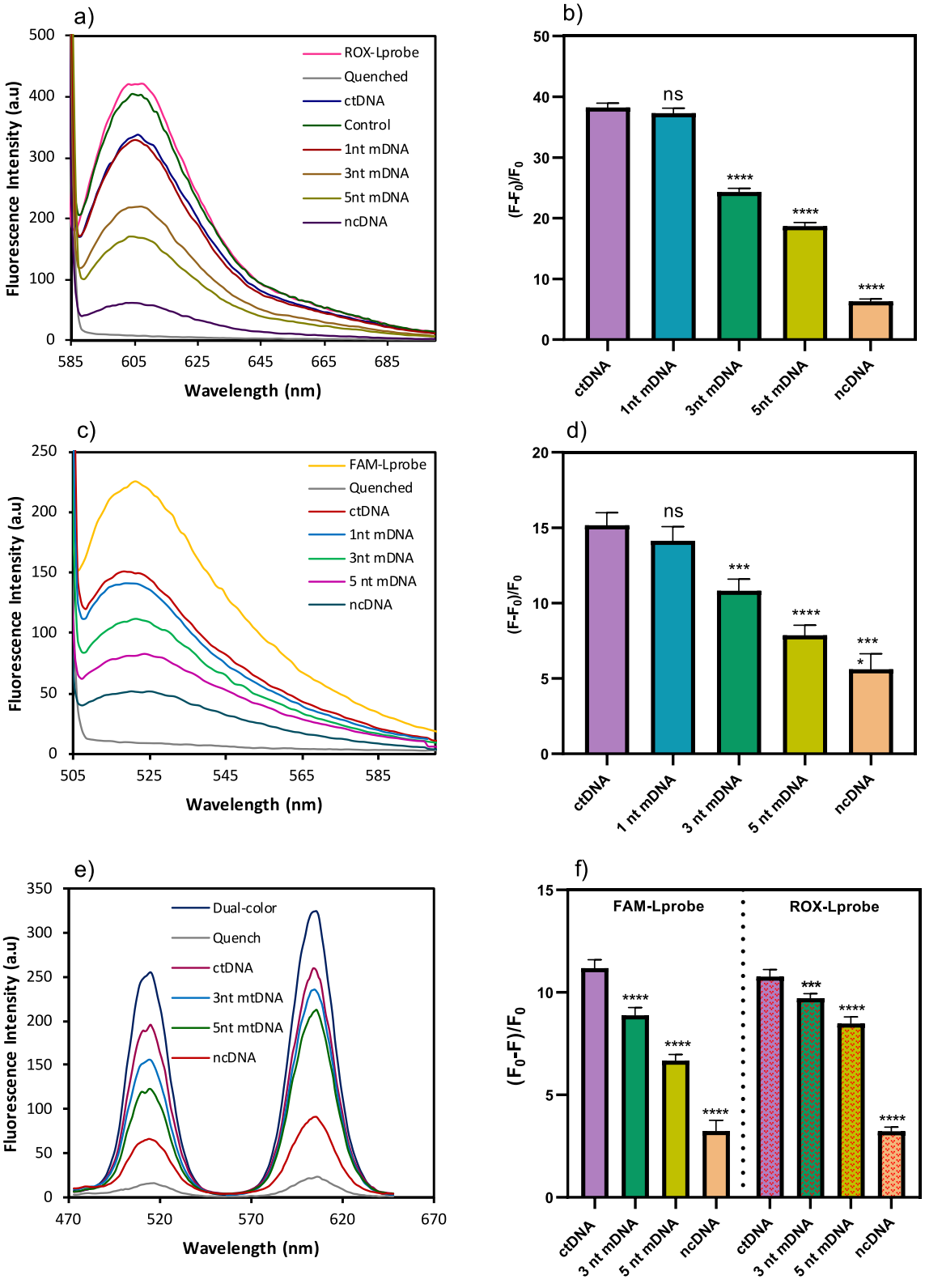

(caption on next page)

Fig. 4. Analysis of the Selectivity of the Biosensor. Fluorescence spectra for determination of the specificity and selectivity of the a) ROX-Lprobe, b) FAM-Lprobe, and c) dual-color biosensor in the presence of single-, three-, and five-mismatch DNA targets. Non-parametric one-way ANOVA test was performed for statistical analysis. Error bars represent mean ± SD. *P < 0.05, **P < 0.01, ***P < 0.001 and ****P < 0.0001. (For interpretation of the references to color in this figure legend, the reader is referred to the Web version of this article.)

N = 3) for ROX-Lprobe (i.e. *SRY* biosensor) and 7.6 nM (S/N = 3) for FAM-Lprobe (i.e. *DYS14* biosensor) (Fig. 3a–d). Table 2 provides the calibration, sensitivity, and specificity of the biosensor following each stage of optimization.

We next investigated whether it is possible to simultaneously detect the ctDNA of both *SRY* and *DYS14* markers in a homogeneous solution using our two-color fluorescent biosensing platform. As shown in Fig. 3e, in the absence of ctDNA, the fluorescence emission intensity of the two fluorophores was negligible, as the fluorophores were quenched by MWCNTs. However, in the presence of ctDNA, the fluorescence emission intensity of the single biosensors i.e. ROX-*SRY* biosensor and FAM-*DYS14* biosensor was significantly enhanced (Fig. 3a–c). Upon the simultaneous addition of the ctDNA of both markers, we observed a clear increase in the fluorescence emission intensity of the dual biosensor (Fig. 3e), which indicates that the ROX- and FAM-labeled probes could properly hybridize to their respective ctDNA and form a duplex DNA structure, which is then released from the MWCNT surface to promote an increase in the fluorescence signal. Thus, our dual-color fluorescence biosensor, which uses both stem-loop and linear probes, allows for the simultaneous, quantitative detection of the *SRY* and *DYS14* ctDNA molecules. We next sought to characterize the two-color fluorescent biosensor, and found that the optimal incubation time for the simultaneous hybridization of ROX- and FAM-labeled probes with ctDNA was 16 min (Fig. S3). Moreover, when the concentrations of the dual ctDNA molecules were increased, a higher fluorescent signal was detected for in each of the two fluorophores (Fig. 3e), which suggests that a higher amount of dsDNA was formed and then released from the MWCNT surface. We determined that the LOD of the dual biosensor was 5.4 nM (ROX-Lprobe), and 9.2 nM (FAM-Lprobe) (Fig. 3e). Finally, our dynamic range estimation experiments revealed that the dynamic range of the dual biosensor was between 40 nM and 1 μM (Fig. 3e and f).

When we used three- or five-mismatch DNA targets, only a 21.2-fold or 8.4-fold fluorescence increase was observed for the ROX-Lprobe (Fig. 4a and b) or the FAM-Lprobe (Fig. 4c and d), respectively. In contrast, ctDNAs with perfectly matched sequences induced a 42-fold (ROX-Lprobe) or 20-fold (FAM-Lprobe) enhancement in the fluorescence intensity (Fig. 4a–d). For the dual biosensor, we found a 27.2- (ROX) or 12.2-fold increase (FAM) in the fluorescence emission intensity (Fig. 4e and f), which was a much smaller increase compared to the fluorescence increase by the perfectly-matched DNA targets. These findings indicate that our sensing platform could efficiently distinguish between completely matched and mismatched DNA targets. These collective data indicate that our dual sensing platform is both specific and sensitive in simultaneously detecting the *SRY* and *DYS14* biomarkers in a homogenous solution.

3.4. The dual biosensor accurately detects SRY and DYS14 DNA biomarkers in real maternal plasma samples

Next, to evaluate the applicability of our sensing system in real samples, we repeated our experiments in maternal blood plasma instead of ctDNA. As shown in Fig. 5a and b, cffDNA extracted from maternal plasma was detected by traditional PCR and qPCR specific for *SRY* and *DYS14* genes. First, cffDNA were treated with 60% DMSO for 2 min to ensure the complete denaturation of maternal dsDNA molecules into ssDNA. We used DMSO for dsDNA denaturation because it decreases the melting temperature (Tm) of the DNA [34]. As shown in Fig. 5c and d, we observed good recovery of cffDNA between 38.76% and 42.71% for individual FAM--*DYS14* and ROX-*SRY* biosensors, respectively.

Finally, the maternal plasma samples were also investigated by using the dual-color biosensor. The synchronous scanning fluorescence spectra indicated that simultaneous detection using our dual biosensor had an efficiency of 39.21% (ROX) and 34.28% (FAM) (Fig. 5h), which shows a similar efficiency to similarly designed dual biosensors [35,36]. Therefore, the results indicated that proposed DNA biosensor could be used for *SRY* gene and *DYS14* marker detection in plasma matrices. Most of the studies conducted so far have detected the *SRY* gene alone or the *DYS14* marker using free fetal DNA [16,17,37]. In this work, both of these markers were detected simultaneously in the optimal time of 28 min with this sensing platform. The specificity and accuracy of this biosensor were confirmed in the presence of DNA targets mixture (ctDNA for *SRY* and *DYS14*), so that by using the stem-loop-probe-based fluorescent DNA sensors in this assay, we were able to partially prevent incomplete hybridizations in the mixture of DNA targets. The actual sex of the future newborns and the outcomes of diagnosis are reported in Table S1 for all samples, listed in a decreasing order according to the gestational week.

3.5. Comparison of the fabricated fluorescent biosensor with other methods for cffDNA detection

Finally, we went on to compare our biosensing platform with some other reported biosensors that have tried to detect cffDNA. Table 3 provides the efficiency of our proposed method, including LOD, linear range, and response time of other biosensing approaches for the determination of cffDNA in maternal plasma. As is evident from the table, our single and dual nanobiosensors showed appropriate LODs, linear ranges, and response time compared to other single biosensors previously reported [16,17,37,38]. Our simple fluorescence approach for *SRY* and *DYS14* detection exhibits an acceptable linear range and a LOD comparable to other fluorescent approaches [35,36]. In particular, the response time of the fabricated biosensors was comparably short including for the dual biosensor (12–16 min; Table 3).

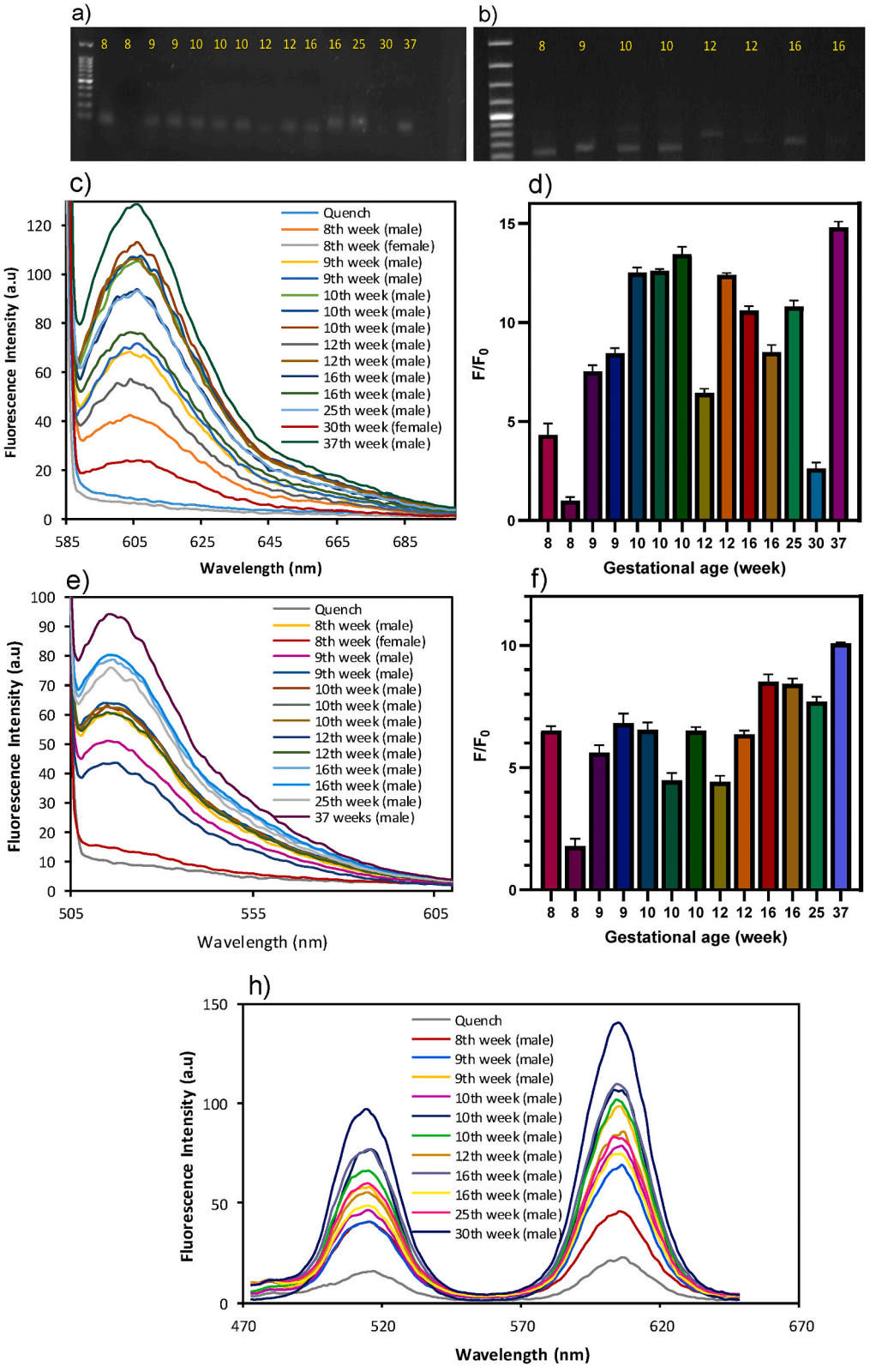

(caption on next page)

Fig. 5. Detection of *SRY* and *DYS14* in Real Maternal Samples using the Proposed Biosensing Platform. Agarose gel electrophoresis pattern of (a) *SRY* and (b) *DYS14* in real samples. (c) Fluorescence spectra for evaluation of the applicability of the biosensor for the detection of *SRY* marker. (d) Bar graph representing changes in the relative emission intensity of *SRY* in real samples. (e) Fluorescence spectra for evaluation of the applicability of the biosensor for the detection of *DYS14* markers. (f) Bar graph representing changes in the relative emission intensity of *DYS14* in real samples. (h) Fluorescence spectra for evaluation of the applicability of the biosensor for the detection of simultaneously in real maternal samples.

Table 3
Comparison of our biosensor with other reported biosensors for cffDNA determination.

Methods	Single or dual detection	Linear range	LOD	Response time	Ref.
Electrochemical biosensor: modified electrode (PANi–RGO–G*NPs/Au)	Single	1.0×10^{-16} -1.0×10^{-8} M	4.26×10^{-17} M	Not mentioned	[16]
Electrochemical biosensor: modified electrode (GCE/RGO)	Single	1.0×10^{-20}-1.0×10^{-14} M	3.2×10^{-21} M	70 min	[38]
Fluorescence nanobiosensor: modified graphene quantum dots-HTAB	Single	1.6×10^{-20} - 1.5×10^{-29} M	8.2×10^{-21} M	20–25 min	[17]
Electrochemical biosensor: modified electrode (Cu (OH)2 @N–C n-boxes)	Single	5×10^{-26}-5×10^{-24} M	1.6×10^{-16} M	3h	[37]
Single *SRY*-ROX fluorescent DNA biosensor	Single	1.0×10^{-8} -1.0×10^{-7} M	4.5×10^{-10} M	13 min	This study
Single *DYS14*-FAM fluorescent DNA biosensor	Single	2.0×10^{-8} -9.0×10^{-7} M	7.6×10^{-10} M	12 min	This study
Dual fluorescent DNA biosensor	Dual	1.0×10^{-8} -1.0×10^{-2} M	5.4×10^{-9} M, 9.2×10^{-9} M	28 min	This study

4. Conclusion

cffDNA detection for sex determination is a non-invasive method used to determine the sex of a fetus during pregnancy. The common methods used to detect cffDNA for sex determination include qPCR, digital PCR, and next-generation sequencing (NGS). PCR-based methods are highly sensitive and specific for amplifying and detecting specific DNA sequences, including cffDNA. They offer straightforward protocols for amplifying target sequences, making them suitable for high-throughput analyses. However, they are relatively expensive and require a skilled person and advanced equipment to perform it [39,40]. NGS allows for comprehensive analysis of cffDNA, including detection of chromosomal abnormalities and genetic variants but requires complex and expensive instrumentation and bioinformatics analysis, limiting its accessibility and scalability for routine clinical use; moreover, it has longer turnaround times compared to sensor-based methods [41]. Our biosensor-based method offers several advantages over other techniques for the detection and measurement of cffDNA in terms of rapid, low-tech, versatile, easy-to-use, and multiplexing capability making it a valuable tool for prenatal diagnostics and research [42]. In this work, a fluorescence sensing platform was developed for the detection of cffDNA in maternal plasma for fetal sex determination. Toward this goal, ROX (i.e. *SRY*-specific probes) and FAM (i.e. *DYS14*-specific probes) fluorophores were used to label ssDNA probes, and MWCNT nanomaterials were employed as nano-quenchers. In the presence of MWCNTs, fluorescence emission of ROX/FAM-Lprobe was quenched due to the quenching feature of MWCNTs. In contrast, when ctDNA was added to the ssDNA-MWCNT conjugates, the fluorescence emission was significantly recovered to 79.5% for ROX-labeled probes (i.e. *SRY*-specific probes), 81.5% for FAM-labeled probes (i.e. *DYS14*-specific probes), and 65.9% for dual-fluorophore biosensor compared to the quenching mode. The linear dynamic range of detection was determined to be 10−1000 nM for ROX-*SRY* biosensor and 20−1000 nM for FAM-*DYS14* biosensor, with their LODs being 4.5 and 7.6 nM, respectively. We suggest that this biosensing platform offers several advantages. This method can avoid the interference of the Raleigh light scattering signal with the fluorescence signal of dyes, improving the detection sensitivity, and can be conducted in a complex system. It can also eliminate the need for multiple-laser excitation sources [43]. Due to planar structure and easy operation of MWCNTs, the proposed method allows MWCNTs to adsorb various kinds of DNA probes. In summary, the results of this study indicate that the proposed sensing platform has the potential to be used as a high-selectivity, highly-sensitive, multiplex, and cost-effective system for detecting cffDNA in fetal sex determination settings. Although the obtained results indicate that high sensitivity and specificity toward detecting specific *SRY* and *DYS14* sequences is possible, further optimizations e.g., optimized immobilization and hybridization need to be performed.

Declarations

The study was approved by the Ethics Committee of the Royan Institute, Tehran, Iran (ethics approval ID: IR.ACECR.ROYAN.REC.3198.158).

Data availability

All the data obtained in this study are included in the article and its associated supplementary file.

CRediT authorship contribution statement

Saeed Mohebbi: Writing – original draft, Methodology, Investigation, Conceptualization. **Sheida Zoughi:** Software, Methodology, Data curation. **Farnoush Faridbod:** Writing – review & editing, Project administration, Investigation, Data curation. **Sharif Moradi:** Writing – review & editing, Supervision, Resources, Project administration, Funding acquisition, Conceptualization.

Declaration of competing interest

The authors declare that they have no known competing financial interests or personal relationships that could have appeared to influence the work reported in this paper.

Acknowledgments

We would like to thank Mohammad Ali Heidarnia, director of the NIGEB's Department of Specialized Services, for his administrative assistance and providing lab space. This work was performed at miRas Biotech, Tehran, Iran.

Appendix A. Supplementary data

Supplementary data to this article can be found online at https://doi.org/10.1016/j.heliyon.2024.e33131.

References

[1] K.M. Finning, L.S. Chitty, Non-invasive fetal sex determination: impact on clinical practice, in: Seminars in Fetal and Neonatal Medicine, 13, Elsevier, 2008, pp. 69–75.
[2] B. Levy, M. Stosic, Traditional prenatal diagnosis: past to present, Prenat. Diagn. (2019) 3–22.
[3] K. Miura, A. Higashijima, T. Shimada, S. Miura, K. Yamasaki, S. Abe, O. Jo, A. Kinoshita, A. Yoshida, S. Yoshimura, Clinical application of fetal sex determination using cell-free fetal DNA in pregnant carriers of X-linked genetic disorders, J. Hum. Genet. 56 (4) (2011) 296–299.
[4] A. Tabor, Z. Alfirevic, Update on procedure-related risks for prenatal diagnosis techniques, Fetal Diagn. Ther. 27 (1) (2010) 1–7.
[5] M. Odeh, V. Grinin, M. Kais, E. Ophir, J. Bornstein, Sonographic fetal sex determination, Obstet. Gynecol. Surv. 64 (1) (2009) 50–57.
[6] Y.D. Lo, N. Corbetta, P.F. Chamberlain, V. Rai, I.L. Sargent, C.W. Redman, J.S. Wainscoat, Presence of fetal DNA in maternal plasma and serum, The lancet 350 (9076) (1997) 485–487.
[7] T. Everett, L. Chitty, Cell-free fetal DNA: the new tool in fetal medicine, Ultrasound Obstet. Gynecol. 45 (5) (2015) 499.
[8] R.W. Chiu, Y.D. Lo, Cell-free fetal DNA coming in all sizes and shapes, Prenat. Diagn. 41 (10) (2021) 1193–1201.
[9] Y. Li, B. Zimmermann, C. Rusterholz, A. Kang, W. Holzgreve, S. Hahn, Size separation of circulatory DNA in maternal plasma permits ready detection of fetal DNA polymorphisms, Clin. Chem. 50 (6) (2004) 1002–1011.
[10] F.M. Lun, R.W. Chiu, K. Allen Chan, T. Yeung Leung, T. Kin Lau, Y. Dennis Lo, Microfluidics digital PCR reveals a higher than expected fraction of fetal DNA in maternal plasma, Clin. Chem. 54 (10) (2008) 1664–1672.
[11] H. Masuzaki, K. Miura, K. Yoshiura, S. Yoshimura, N. Niikawa, T. Ishimaru, Detection of cell free placental DNA in maternal plasma: direct evidence from three cases of confined placental mosaicism, J. Med. Genet. 41 (4) (2004) 289–292.
[12] B. Hanson, E. Scotchman, L.S. Chitty, N.J. Chandler, Non-invasive prenatal diagnosis (NIPD): how analysis of cell-free DNA in maternal plasma has changed prenatal diagnosis for monogenic disorders, Clin. Sci. 136 (22) (2022) 1615–1629.
[13] A. Bustamante-Aragones, C. Gonzalez-Gonzalez, M.R. De Alba, E. Ainse, C. Ramos, Noninvasive prenatal diagnosis using ccffDNA in maternal blood: state of the art, Expert Rev. Mol. Diagn. 10 (2) (2010) 197–205.
[14] K.L. Johnson, K.A. Dukes, J. Vidaver, E.S. LeShane, I. Ramirez, W.D. Weber, F.Z. Bischoff, S. Hahn, A. Sharma, D.X. Dang, Interlaboratory comparison of fetal male DNA detection from common maternal plasma samples by real-time PCR, Clin. Chem. 50 (3) (2004) 516–521.
[15] M. Calcagno, R. D'Agata, G. Breveglieri, M. Borgatti, N. Bellassai, R. Gambari, G. Spoto, Nanoparticle-enhanced surface plasmon resonance imaging enables the ultrasensitive detection of non-amplified cell-free fetal DNA for non-invasive prenatal testing, Anal. Chem. 94 (2) (2021) 1118–1125.
[16] M. Malmir, J. Arjomandi, A.G. Khosroshahi, M. Moradi, H. Shi, Label-free E-DNA biosensor based on PANi-RGO-G* NPs for detection of cell-free fetal DNA in maternal blood and fetal gender determination in early pregnancy, Biosens. Bioelectron. 189 (2021) 113356.
[17] M. Rahaie, B. Ostad-Hasanzadeh, F. Faridbod, A novel fluorescence nanobiosensor based on modified graphene quantum dots-HTAB for early detection of fetal sexuality with cell free fetal DNA, J. Fluoresc. 31 (2021) 1843–1853.
[18] C.M. Stawicki, T.E. Rinker, M. Burns, S.S. Tonapi, R.P. Galimidi, D. Anumala, J.K. Robinson, J.S. Klein, P. Mallick, Modular fluorescent nanoparticle DNA probes for detection of peptides and proteins, Sci. Rep. 11 (1) (2021) 19921.
[19] X. Su, X. Xiao, C. Zhang, M. Zhao, Nucleic acid fluorescent probes for biological sensing, Appl. Spectrosc. 66 (11) (2012) 1249–1262.
[20] A.H. Loo, Z. Sofer, D. Bouša, P. Ulbrich, A. Bonanni, M. Pumera, Carboxylic carbon quantum dots as a fluorescent sensing platform for DNA detection, ACS Appl. Mater. Interfaces 8 (3) (2016) 1951–1957.
[21] R. Yang, J. Jin, Y. Chen, N. Shao, H. Kang, Z. Xiao, Z. Tang, Y. Wu, Z. Zhu, W. Tan, Carbon nanotube-quenched fluorescent oligonucleotides: probes that fluoresce upon hybridization, J. Am. Chem. Soc. 130 (26) (2008) 8351–8358.
[22] D.P. Kalogianni, Nanotechnology in emerging liquid biopsy applications, Nano convergence 8 (1) (2021) 13.
[23] H. Li, Y. Zhang, Y. Luo, X. Sun, Nano-C60: a novel, effective, fluorescent sensing platform for biomolecular detection, Small 7 (11) (2011) 1562–1568.
[24] R. Yang, Z. Tang, J. Yan, H. Kang, Y. Kim, Z. Zhu, W. Tan, Noncovalent assembly of carbon nanotubes and single-stranded DNA: an effective sensing platform for probing biomolecular interactions, Anal. Chem. 80 (19) (2008) 7408–7413.
[25] C.H. Lu, H.H. Yang, C.L. Zhu, X. Chen, G.N. Chen, A graphene platform for sensing biomolecules, Angew. Chem. 121 (26) (2009) 4879–4881.
[26] B. Dubertret, M. Calame, A.J. Libchaber, Single-mismatch detection using gold-quenched fluorescent oligonucleotides, Nat. Biotechnol. 19 (4) (2001) 365–370.
[27] D.J. Maxwell, J.R. Taylor, S. Nie, Self-assembled nanoparticle probes for recognition and detection of biomolecules, J. Am. Chem. Soc. 124 (32) (2002) 9606–9612.
[28] X. Zhu, H. Zheng, X. Wei, Z. Lin, L. Guo, B. Qiu, G. Chen, Metal–organic framework (MOF): a novel sensing platform for biomolecules, Chem. Commun. 49 (13) (2013) 1276–1278.
[29] N. Nakayama-Ratchford, S. Bangsaruntip, X. Sun, K. Welsher, H. Dai, Noncovalent functionalization of carbon nanotubes by fluorescein– polyethylene glycol: supramolecular conjugates with pH-dependent absorbance and fluorescence, J. Am. Chem. Soc. 129 (9) (2007) 2448–2449.

[30] S. Kumar, R. Rani, N. Dilbaghi, K. Tankeshwar, K.-H. Kim, Carbon nanotubes: a novel material for multifaceted applications in human healthcare, Chem. Soc. Rev. 46 (1) (2017) 158–196.
[31] Y. Yang, Y. Xiao, M. Li, F. Ji, C. Hu, Y. Cui, Evaluation of complex toxicity of canbon nanotubes and sodium pentachlorophenol based on earthworm coelomocytes test, PLoS One 12 (1) (2017) e0170092.
[32] C. Li, G. Shi, Carbon nanotube-based fluorescence sensors, J. Photochem. Photobiol. C Photochem. Rev. 19 (2014) 20–34.
[33] S. Jung, M. Cha, J. Park, N. Jeong, G. Kim, C. Park, J. Ihm, J. Lee, Dissociation of single-strand DNA: single-walled carbon nanotube hybrids by Watson− Crick base-pairing, J. Am. Chem. Soc. 132 (32) (2010) 10964–10966.
[34] X. Wang, H.J. Lim, A. Son, Characterization of denaturation and renaturation of DNA for DNA hybridization, Environmental health and toxicology 29 (2014).
[35] O. Hu, Z. Li, Y. Tong, Q. Wang, Z. Chen, DNA functionalized double quantum dots-based fluorescence biosensor for one-step simultaneous detection of multiple microRNAs, Talanta 235 (2021) 122763.
[36] Y. Zheng, J. Chen, Y. Li, Y. Xu, L. Chen, W. Chen, A. Liu, X. Lin, S. Weng, Dual-probe fluorescent biosensor based on T7 exonuclease-assisted target recycling amplification for simultaneous sensitive detection of microRNA-21 and microRNA-155, Anal. Bioanal. Chem. 413 (2021) 1605–1614.
[37] P. Tahmasebi, S. Farokhi, G. Ahmadi, M. Roushani, Electrochemical impedance biosensor based on Y chromosome–specific sequences for fetal sex determination, Microchim. Acta 190 (12) (2023) 483.
[38] A. Benvidi, N. Rajabzadeh, M. Mazloum-Ardakani, M.M. Heidari, A. Mulchandani, Simple and label-free electrochemical impedance Amelogenin gene hybridization biosensing based on reduced graphene oxide, Biosens. Bioelectron. 58 (2014) 145–152.
[39] G. Gullo, M. Scaglione, G. Buzzaccarini, A.S. Laganà, G. Basile, V. Chiantera, G. Cucinella, S. Zaami, Cell-free fetal DNA and non-invasive prenatal diagnosis of chromosomopathies and pediatric monogenic diseases: a critical appraisal and medicolegal remarks, J. Personalized Med. 13 (1) (2022) 1.
[40] Y.D. Lo, Discovery of cell-free fetal DNA in maternal blood and development of noninvasive prenatal testing: 2022 lasker-DeBakey clinical medical research award, JAMA 328 (13) (2022) 1293–1294.
[41] X.-P. Xu, H.-Y. Gan, F.-X. Li, Q. Tian, J. Zhang, R.-L. Liang, M. Li, X.-X. Yang, Y.-S. Wu, A method to quantify cell-free fetal DNA fraction in maternal plasma using next generation sequencing: its application in non-invasive prenatal chromosomal aneuploidy detection, PLoS One 11 (1) (2016) e0146997.
[42] S. Sadeghi, M. Rahaie, B. Ostad-Hasanzadeh, Nanostructures in non-invasive prenatal genetic screening, Biomedical Engineering Letters 12 (1) (2022) 3–18.
[43] Q. Zhu, D. Xiang, C. Zhang, X. Ji, Z. He, Multicolour probes for sequence-specific DNA detection based on graphene oxide, Analyst 138 (18) (2013) 5194–5196.